Magnetic anisotropies effect on the Spin-Seebeck response in spinel ferrite thin films

J. Gil-Monsalve[1], A. I. Figueroa[2], G. van der Laan[3], G. Campillo[4], Alpha T. N'Diaye[5] C. Ostos[6], A. Azevedo[7], O. Arnache[1]

[1]Instituto de Física. Universidad de Antioquia. Medellín-Colombia
[2]Departament de Física de la Matèria Condensada and Institut de Nanociència i Nanotecnologia, Universitat de Barcelona, Barcelona, Spain.
[3]Magnetic Spectroscopy Group, Diamond Light Source, UK
[4]Facultad de Ciencias Básicas, Universidad de Medellín. Medellín-Colombia
[5]Advanced Light Source, Lawrence Berkeley National Laboratory, Berkeley, CA, USA
[6]Plataforma NAP-XPS, Universidad de Antioquia, Medellín, Colombia
[7]Departamento de Física, Universidade Federal de Pernambuco, Recife, Brazil.
johanna.gilm@udea.edu.co

UNIVERSIDAD DE ANTIOQUIA 1803

GES Grupo de Estado Sólido

Introduction

Observation of spin Seebeck effect (SSE) at room temperature in a weak ferromagnetic material, for example, a spinel zinc ferrite ($ZnFe_2O_4$) in bulk and thin film is demonstrated. In order to understand the physics behind this effect, a systematic structural and magnetic characterization with the SSE signal in this ferrite is presented. Measurements of surface analysis by x-ray photoemission (XPS) and absorption (XAS) spectroscopies, and x-ray magnetic circular dichroism (XMCD) provide information about the cationic distribution in the lattice, which is found to be responsible of the magnetic response in the material. The magnetic anisotropy, as well as the Gilbert constant of the ferrite have been investigated by means of ferromagnetic resonance measurements. These measurements are useful to predict the spin Seebeck response in the material.

Experimental process

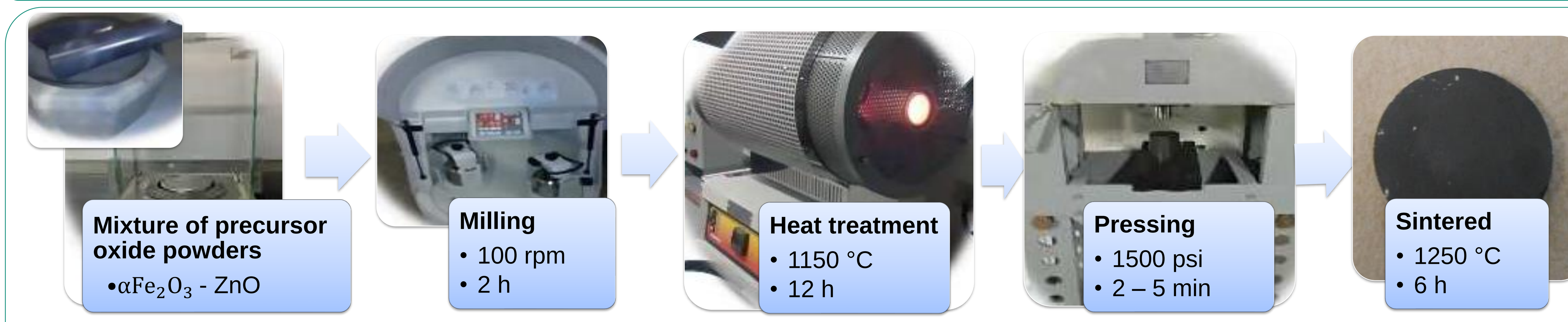

Fig. 1. ZFO target preparation process.

Growth conditions thin films

ZFO thin films were grown using RF magnetron sputtering.

Gas pressure	Growth temperature	Ar/O_2 ratio	Thickness
27 mTorr	500 °C	2:1	90 nm

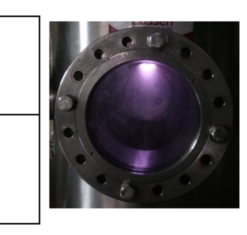

Results

STRUCTURAL CHARACTERIZATION

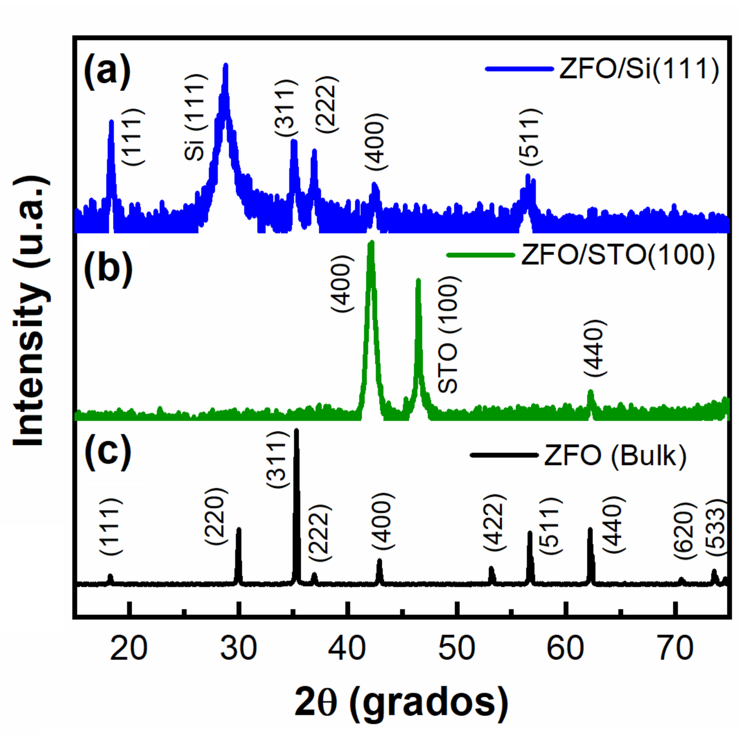

Sample	Lattice parameter
$ZnFe_2O_4$ (Bulk)	8.44 Å
Thin film	8.43 Å

Fig. 2. XRD patterns of the $ZnFe_2O_4$ in bulk and ZFO thin films on Si (111) and STO (100) substrates growth under Ar/O_2 - 1:2

MAGNETIC CHARACTERIZATION

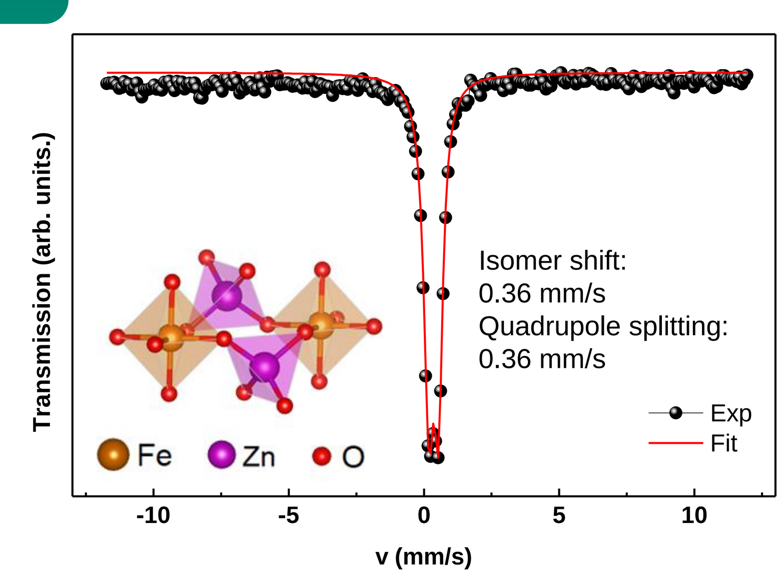

Fig. 3. Mössbauer spectra of ZFO in bulk. The red line corresponds to a fitting of the experimental data using the Recoil software.

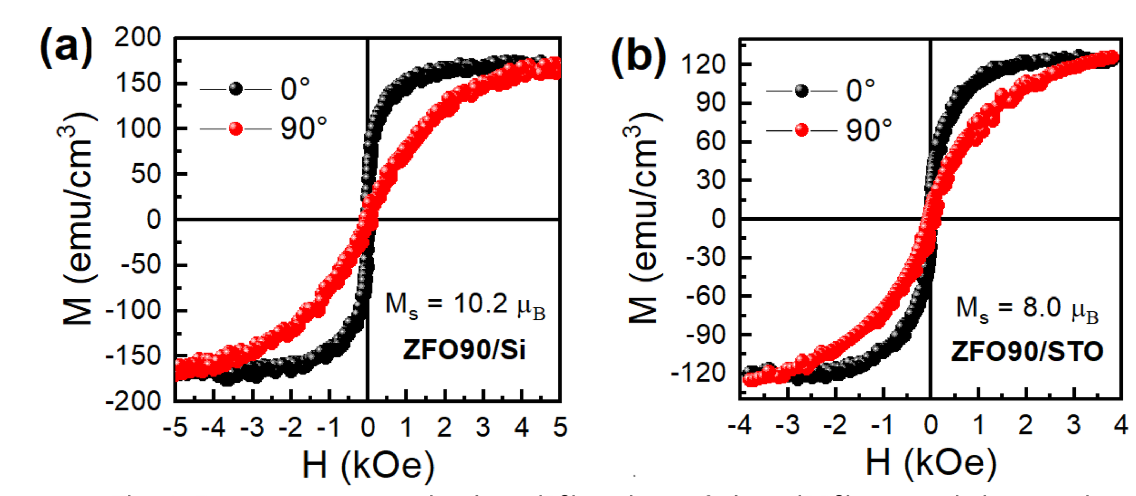

Fig. 4. Room temperature in-plane (0°) and out of plane (90°) magnetic hysteresis loops of ZFO thin films.

Corresponding to characteristic Fe^{3+} charge state in a direct spinel structure.

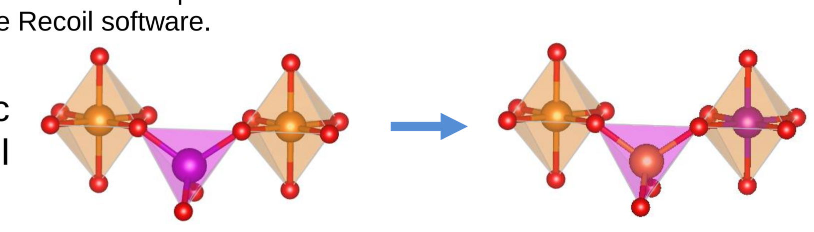

Superexchange interaction
A-O-B (J_{AB}) is the strongest,
B-O-B (J_{BB}) is weaker,
A-O-A (J_{AA}) is the weakest.

XPS ANALYSIS

ZFO/Si

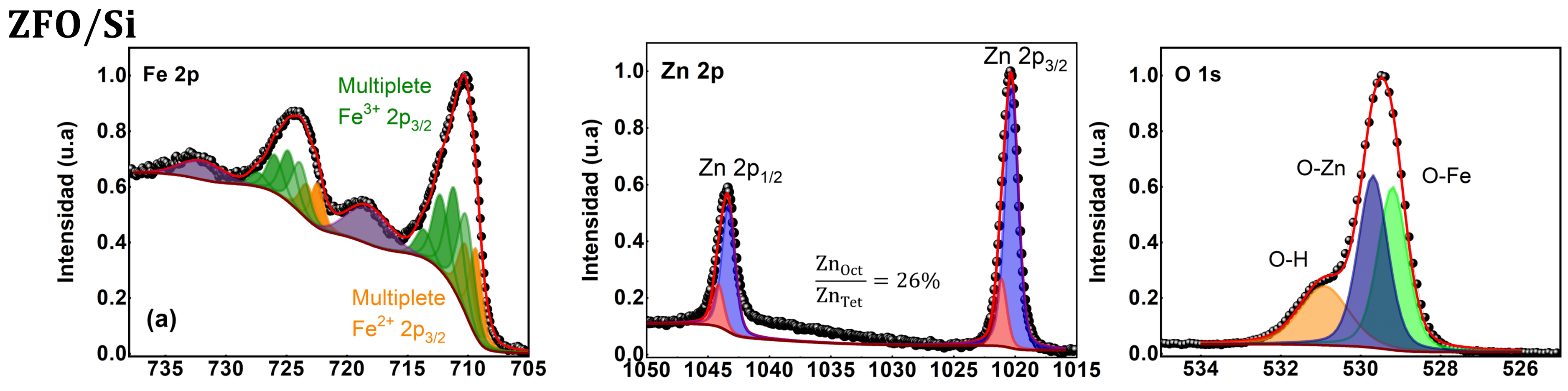

ZFO/STO

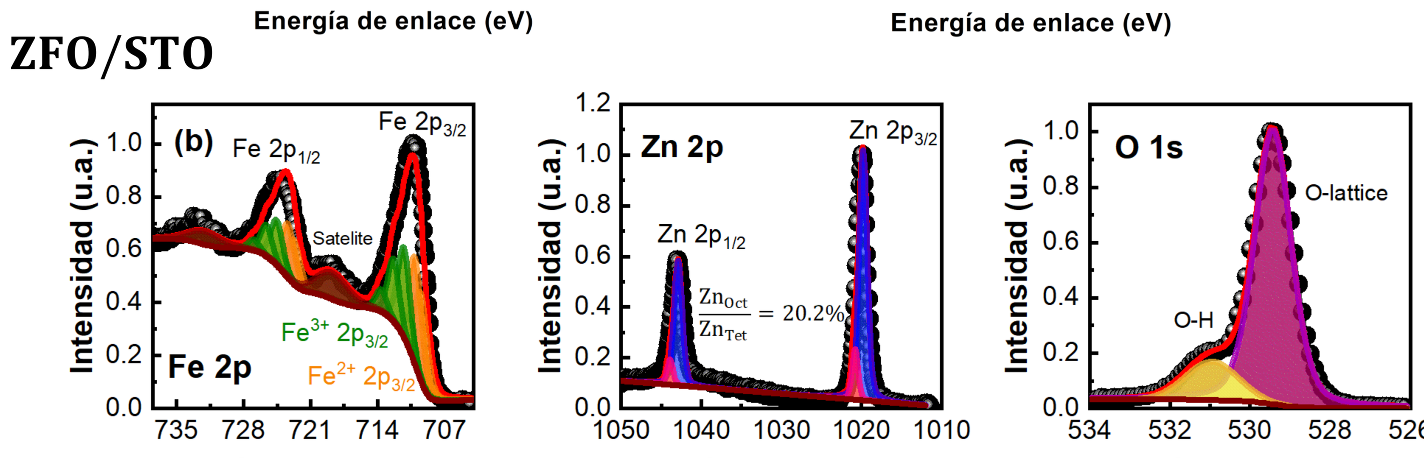

Sample	Fe/Zn atomic ratio	O/Zn atomic ratio
ZFO/Si	1.98	8.74
ZFO/STO	1.87	5.41

Fig. 5. a) XPS spectra for the thin films (a) ZFO/Si(111) (b) ZFO/STO(100). Symbols represent experimental data and lines represent the fit.

XAS AND XMCD ANALYSIS

XAS and XMCD measurements were performed on beamline 6.3.1 at the Advanced Light Source (Berkeley, USA). Technical details of the measurements: energies around Fe L2,3 edges, temperature of 300 K, magnetic field of ± 1 T applied at 30º from the sample plane, detection method was total electron yield.

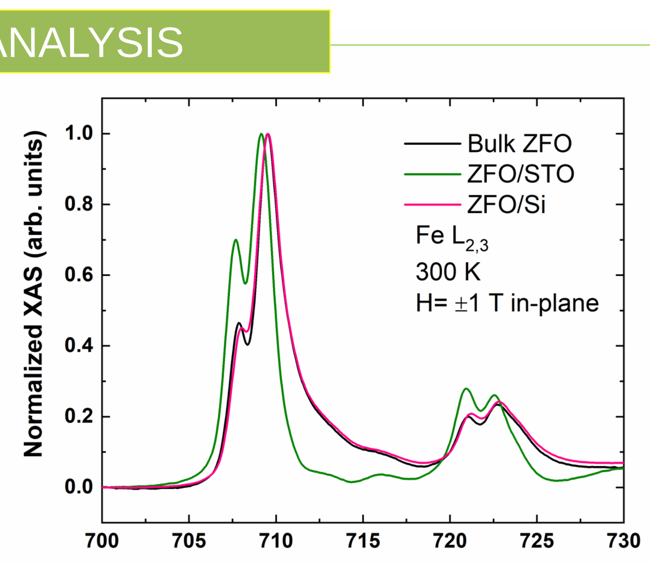

Fig. 6. Comparison of the normalized XAS for the bulk ZFO sample and the thin films grown on Si and STO. An evident shift towards lower energies, indicative of a lower valence (e.g Fe^{2+}), is observed on the ZFO/STO sample.

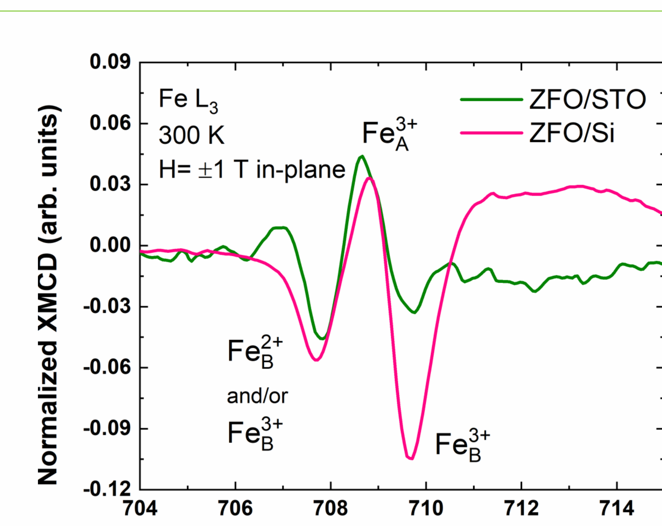

Fig. 7. Normalized XMCD results for the ZFO/Si and ZFO/STO thin films. A larger width is observed for ZFO/Si, consistent with a higher value of magnetization for that sample. The intensity is more pronounced for the sites occupied by Fe^{3+} in octahedral environment, suggesting a larger component for this sample.

FERROMAGNETIC RESONANCE

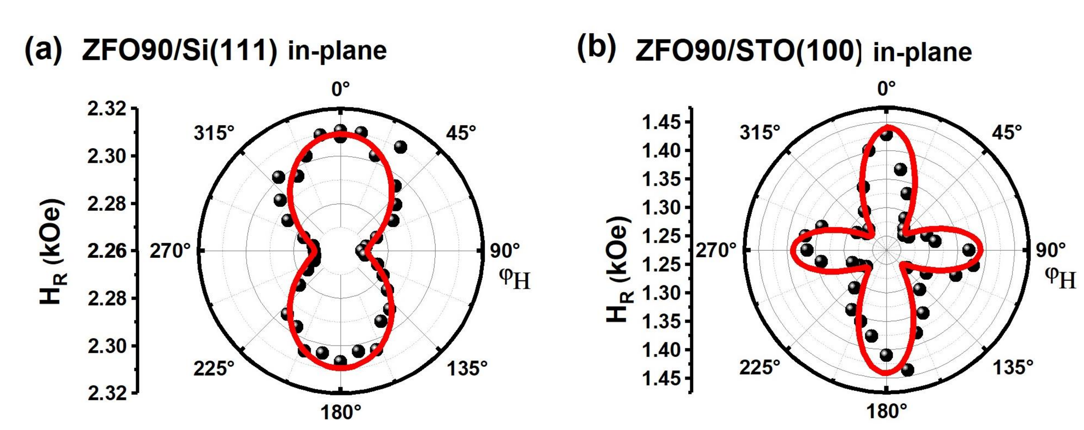

	ZFO/Si	ZFO/STO
$4\pi M_s$ (Oe)	1791.0	1587.0
$H_\perp$ (Oe)	-2200.0	-1484.7
H_c (Oe)		90.7
$H_\parallel$ (Oe)	-28.8	-29.0

Fig. 8. Ferromagnetic resonance field as a function of the in-plane azimuthal angle φ_H for ZFO/Si and ZFO/STO. The red solid lines are theoretical fits to the experimental data (black spheres).

LONGITUDINAL SPIN SEEBECK EFFECT

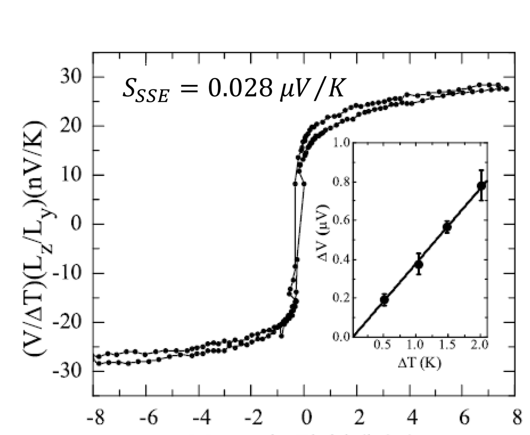

Fig. 9. SSE response with applied magnetic field. (Inset) ΔT dependence of SSE voltage ΔV [4].

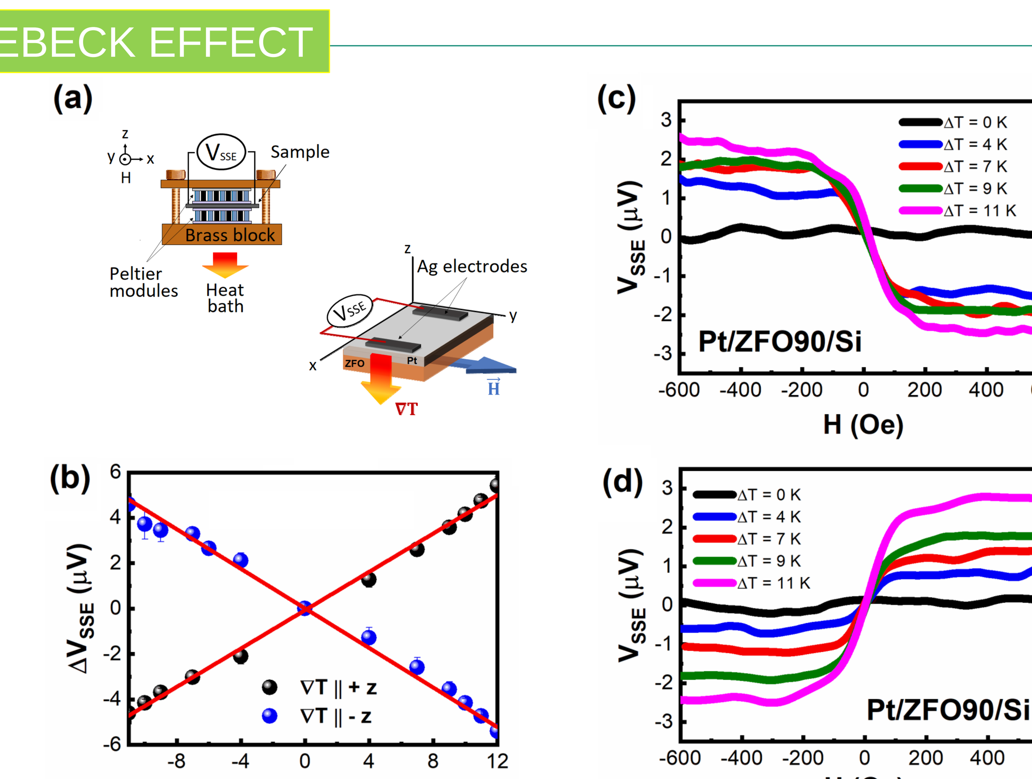

Fig. 10. (a) Schematic illustration of the LSSE experimental set-up. (b) Variation of the voltage with ΔT when the temperature gradient is applied along the +z and -z. (c) and (d) Variation with the magnetic field of the V_{SSE} measured on the Pt layer for different values of ΔT for Pt/ZFO/Si as indicated.

Thin film	S_{SSE} ($\mu V/K$)	κ_{subs} (W/mK)	$\alpha_{Gilbert}$
ZFO/Si	0.003	148	0.022
ZFO/STO	0.11	12	0.035

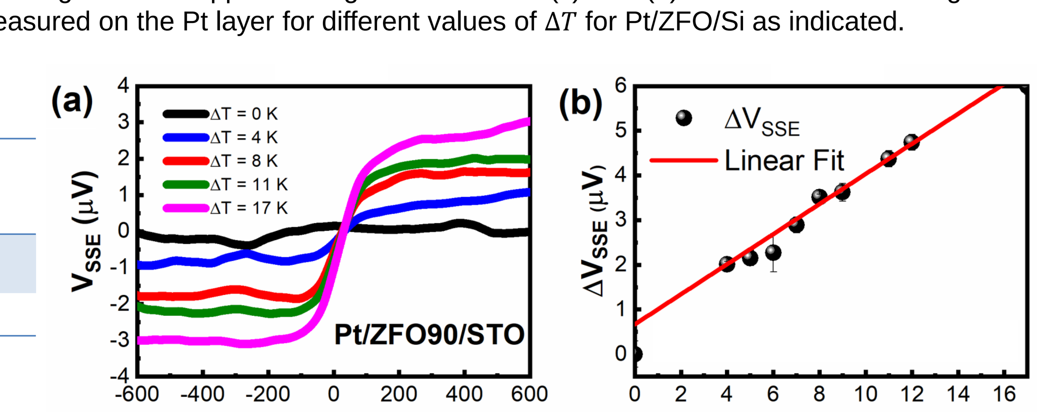

Conclusion

The spin Seebeck coefficients extracted from the data for the thin films were highly sensitive to the thermal conductivity of the thin film and the substrate. Therefore, before measuring the Seebeck response in a material, it is important to pay more attention to the growth of the magnetic layer, and the choice of substrate.

The lattice mismatch and the presence of anisotropies in the sample can significantly change the magnitude of LSSE voltage; also, the type of substrate plays an important role in the calculated spin Seebeck coefficient.

Acknowledgment
This work was supported by Solid State Group - GES at the University of Antioquia in the framework of Sustainability Strategy 2020-2021 and by Colombian Science and technology Ministry (project no. 111580863381). We thank the following Brazilian agencies for partial funding: Conselho Nacional de Desenvolvimento Científico e Tecnológico (CNPq), Coordenação de Aperfeiçoamento de Pessoal de Nível Superior (CAPES), Financiadora de Estudos e Projetos (FINEP), Fundação de Amparo à Ciência e Tecnologia do Estado de Pernambuco (FACEPE). Also, the authors acknowledge beamtime on beamline 6.3.1 of the Advanced Light Source under proposal ALS-10821.

References

[1] Rastogi, A., Li, Z., Singh, A. V., Regmi, S., Peters, T., Bougiatioti, P. & Gupta, A. Physical Review Applied, 14(1), 014014 (2020).
[2] P. Jiménez-Cavero, I. Lucas, D. Bugallo, C. López-Bueno, R. Ramos, P.A. Algarabel, M.R. Ibarra, F. Rivadulla, L. Morellón, Appl. Phys. Lett. 118 (2021).
[3] Gil-Monsalve, J., Abrão, J. E., Santos, E., Ricalde, A., Azevedo, A., & Arnache, O. Physical Review B, 105(1), 014420 (2022).
[4] JD Arboleda, O Arnache and MH Aguirre, Solid State Communications, Vol. 270, p. 140-146 (2018).